Chromium-containing organometallic nanomaterials for non-linear optics†

Larisa G. Klapshina,*[a] Ilya S. Grigoryev,[a] Tatyana I. Lopatina,[a] Vladimir V. Semenov,[a] Georgy A. Domrachev,[a] William E. Douglas,[b] Boris A. Bushuk,[c] Sergei B. Bushuk,[c] Andrey Yu. Lukianov,[d] Andrey V. Afanas'ev,[e] Robert E. Benfield[f] and Alexey I. Korytin[e]

Received (in Montpellier, France) 26th September 2005, Accepted 27th January 2006
First published as an Advance Article on the web 15th February 2006
DOI: 10.1039/b513465j

Novel non-linear optical polymeric film-producing nanocomposites based on bis(arene)chromium complexes incorporated into a CN-containing matrix have been developed. Polymeric nanocomposite precursors were prepared by the reaction of $Cr(Et_nC_6H_{6-n})_2$ (n = 1,2,3) with CN-containing vinyl monomers (acrylonitrile, crotononitrile or ethyl 2-cyanopropenoate). Extraordinarily high third-order non-linear optical susceptibilities of the ultra-fast electronic type have been demonstrated at various wavelengths for polymer films prepared from these composites by using the Z-scan technique and the spectrally-resolved two-beam coupling method. A notable electro-optical response of the composite with an essential contribution of orientational effects was established. The electron-diffraction pattern in films and the presence of a non-zero electro-optical coefficient in the absence of an external poling field indicate the formation of self-organized structures. In CrPAN and $[CrPAN]^+TCNE^-$, a single Cr–C distance was found in the EXAFS data refinement, showing that the arene rings are parallel and symmetric as in bis(benzene)chromium. The Cr–C distances in these two materials are very similar to the 2.13 Å in bis(benzene)chromium. In $[CrPAN]^+OH^-$, more than one metal–carbon distance was resolved, showing either that the two arene rings are at different distances from the metal, or that they are tilted rather than parallel.

Introduction

At the present time, the field of soluble organometallic polymer materials possessing a combination of interesting electronic, magnetic, optical and non-linear optical properties is attracting great attention with the promise of a variety of practical applications. The main interest is in modern information technologies requiring devices for high speed optical information processing where, unlike in analogous electronic devices, light is the controlling factor. The highest speed of information processing can be provided by materials possessing non-linearities with extremely short response times (10^{-14}–10^{-15} s). Such response times are typical of non-linear optical processes determined by the high polarizability of a mobile (diffuse) electron layer present in some organic and organometallic compounds, *e.g.* in π-conjugated polymers and charge transfer complexes with a strong electronic polarization along the metal–ligand charge-transfer axis.

Thus, in our choice of scientific approaches for the formation of non-linear optical structures we expected the most promising to be the incorporation of transition metal atoms or ions into a conjugated polymer chain in the form of a metal complex. Such structures should be able to exhibit the highest optical non-linearities since they combine the advantages of conjugated polymers and charge transfer complexes. The main aim of the present investigations was the preparation of materials with extremely high non-resonant cubic non-linear-optical susceptibilities based on transition metal bis-arene complexes forming π-conjugated polynaphthyridine-type structures in a matrix of a CN-containing polymer.

Previously, we have reported the synthesis of $(arene)_2M$-containing polyacrylonitrile (M = Cr,V) prepared by the polycyanoethylation reaction between bis-arene complexes and acrylonitrile.[1–5] The resulting star-shaped molecules consist of a central $(arene)_2M$ species with polyacrylonitrile (PAN) arms covalently bonded to the arene ligands. The properties of thermolysed bis(arene)metal-containing polyacrylonitrile (MPAN) are consistent with the formation of

[a] *G. A. Razuvaev Institute of Organometallic Chemistry, Russian Academy of Sciences, Tropinin Street 49, GSP-445, 603600 Nizhny Novgorod, Russia. E-mail: klarisa@iomc.ras.ru; Fax: +7 8132 661497; Tel: +7 8132 664370*
[b] *Laboratoire de Chimie Moléculaire et Organisation du Solide (CNRS UMR 5637), Université Montpellier II, Place E. Bataillon, 34095 Montpellier Cedex 5, France*
[c] *B. I. Stepanov Institute of Physics, National Academy of Science of Belarus, F. Skaryna Ave. 68, 220072 Minsk, Belarus*
[d] *Institute of Microstructure Physics, Russian Academy of Sciences, GSP-105, 603950 Nizhny Novgorod, Russia*
[e] *Institute of Applied Physics, Russian Academy of Sciences, Uljanov Street 46, 603600 Nizhny Novgorod, Russia*
[f] *Functional Materials Group, School of Physical Sciences, University of Kent, Canterbury, UK CT2 7NR*

† Electronic supplementary information (ESI) available: ^1H NMR spectrum of CrPAN prepared from bis(benzene)chromium (CD_3CN solution) and the IR spectra of CrPECA and PECA. See DOI: 10.1039/b513465j

conjugated ladder-type polynaphthyridine structures.[3,4] Thus, MPAN turns out to be a promising polymeric nanocomposite precursor for the preparation of non-linear optical structures: the value of electronic n_2 determined by the DFWM and Z-scan technique at 1064 nm with a 6 ns pulse duration for a solution in concentrated H_2SO_4 (1 g l^{-1}) of the Cr- and V-containing polymers pyrolyzed at 350 °C was found to be 0.8×10^{-13} cm^2 W^{-1} and 2.2×10^{-13} cm^2 W^{-1}, respectively.

Here we report the preparation of a variety of new film-producing materials based on unpyrolized MPAN polymeric nanocomposite precursors and the results of our investigations into their fast cubic optical non-linearities and electrooptical properties. For this study, we used the commercial ethyl-substituted chromium sandwich mixture $(Et_nC_6H_{6-n})_2Cr$ (n = 1,2,3) from Strem which offered several advantages over bis(benzene)chromium or bis(mesitylene)chromium *viz*. (1) the mixture is a liquid forming homogeneous solutions with the monomers, (2) the reaction of the mixture with the monomers is very fast and smooth and takes place in almost quantitative yield in the absence of solvent whereas the reaction with bis(benzene)chromium requires prolonged heating and the presence of solvent, (3) the optical quality of the films produced from the commercial mixture is much higher than for those from bis(benzene)chromium or bis(mesitylene)chromium, and (4) as with bis(mesitylene)chromium, the presence of substituted arenes renders possible the determination of the relative loss of aromatic protons from benzene resulting from the polymerization reaction. It should be noted that all the spectral characteristics of the products obtained starting from the commercial Strem mixture are similar to those from bis(benzene)chromium or bis(mesitylene)chromium.

Experimental

Materials and methods

The $(Et_nC_6H_{6-n})_2Cr$ (n = 1,2,3) was a commercial sample supplied by Strem (composition given in Table 1). Tetrahydrofuran was dried and distilled from sodium benzophenone ketyl. The elemental analyses were performed in the Nizhny Novgorod laboratory. Gas-liquid chromatography (GLC) analysis was perfomed by means of a Tsvet-530 gas chromatograph fitted with a 0.3 × 200 cm stainless steel column (packed with 5% SE-30 on Chromatron N-AW-DMCS solid carrier) and equipped with a thermal conductance detector, the carrier gas being helium. IR spectra were recorded on a Specord M80 spectrophotometer as potassium bromide pellets, Nujol mulls or thin films on KBr plates. Electron paramagnetic resonance (EPR) spectra were run on a Bruker ER 200P-SPC instrument. The solution ^1H NMR spectra were recorded on a Bruker DPX200 spectrometer and the solid state CPMAS ^{13}C NMR spectra on a Bruker AM-300 instrument operating at 75.432 MHz. The transmission electron microscopy (TEM) images were taken on a Jeol 1200EX2 instrument. The absorption spectra of the solutions were recorded by using a Cary-500 spectrophotometer. The fluorescence and fluorescence excitation spectra measurements were performed on an SLM-4800 spectrofluorimeter (spectral width of excitation and registration slits were 8 nm and 4 nm, respectively).

Table 1 Arene ligand composition of $(Et_nC_6H_{6-n})_2Cr$

	Arene ligand (mol%)			
Sample	C_6H_6	EtC_6H_5	$Et_2C_6H_4$	$Et_3C_6H_3$
(1)	≪1	62.4	33.0	5.6
(2)	≪1	50.0	42.0	7.5

Syntheses

CrPAN. Distilled acrylonitrile (0.98 ml, 1.49×10^{-2} mol) and $Cr(Et_nC_6H_{6-n})_2$ (550 mg, 1.86×10^{-3} mol) were mixed without solvent in the presence of the electron acceptor TCNE (10^{-3} mol l^{-1}). The mixture was cooled and stirred at room temperature under argon until the reaction product had hardened. To recover the bis(arene)chromium mixture which had not undergone the cyanoethylation reaction, the crude product was washed with degassed THF followed by degassed acetone. All operations were performed under an inert atmosphere. IR (cm^{-1})ν(C≡N): 2250 s, 2190 w. ^1H NMR (DMF-D7): 1.23, 1.27, 2.19, 2.24, 3.57, 7.18, 7.29, 7.43. Elemental analysis Found: C, 70.97; H, 7.00; N, 15.14; Cr, 6.89 (calculated for $Et_2(C_6H_4)CrEt(C_6H_5)(CH_2CHCN)_8$ C, 70.39; H, 6.71; N, 15.64; Cr, 7.26).

CrMePAN. Redistilled crotononitrile (0.6 ml, 7.38×10^{-3} mol) and $Cr(Et_nC_6H_{6-n})_2$ (260 mg, 8.78×10^{-4} mol) were mixed without solvent in the presence of the electron acceptor TCNE (10^{-3} mol l^{-1}). The mixture was cooled and stirred at room temperature under argon for 3 h until the reaction product became viscous. To recover the bis(arene)chromium mixture which had not undergone the cyanoethylation reaction, the crude product was washed with degassed THF and dried under vacuum. The resulting polymer is readily soluble in acetonitrile and dimethylformamide. All operations were performed under an inert atmosphere. IR (cm^{-1}) ν(C≡N): 2245 s, 2215 w. ^1H NMR (DMF-D7): 1.38, 2.15, 2.28, 2.68, 2.85, 3.00, 3.40, 6,76. Elemental analysis Found: C, 70.24; H, 8.02; N, 15.78; Cr, 5.96 (calculated for $Et_2(C_6H_4)$-$CrEt(C_6H_5)(CH_3CHCHCN)_{8.4}$ C, 72.44; H, 7.72; N, 13.75; Cr, 6.09).

CrPECA. Redistilled ethyl 2-cyanopropenoate (ECA) (0.95 ml, 8.07×10^{-3} mol) and $Cr(Et_nC_6H_{6-n})_2$ (300 mg, 1.01×10^{-3} mol) were mixed in the absence of solvent. ECA polymerized almost immediately forming a polymeric phase separated from the chromium complexes. The resulting product was dissolved in distilled, degassed, acetonitrile (5 ml) affording a homogeneous solution. CrPECA was obtained by evaporation of the solvent under vacuum. All operations were performed under an inert atmosphere. IR (cm^{-1}) ν(C≡N): 2250 s, 2292 w. ^1H NMR (DMF-D7): 1.29, 2.12, 2.59, 2.73, 2.89, 3.52, 3.82, 4.28. Elemental analysis Found: C, 60.14; H, 6.72; N, 9.01; O, 20.30; Cr, 3.83 (calculated for $Et_2(C_6H_4)$-$CrEt(C_6H_5)[CH_2C(COOC_2H_5)CN]_8$ C, 61.30; H, 6.19; N, 8.67; O, 19.81; Cr, 4.03).

X-Ray absorption spectroscopy

X-Ray absorption spectra at the Cr K edge (5989 eV) were collected on beamline 7.1 of the CLRC Daresbury

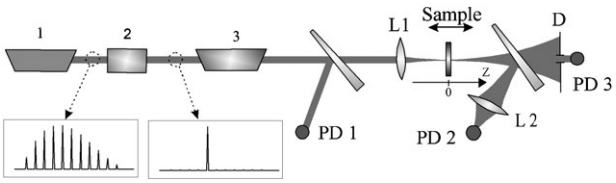

Fig. 1 Experimental setup for Z-scan measurements of non-linear optical susceptibility of polymers with picosecond pulse duration.

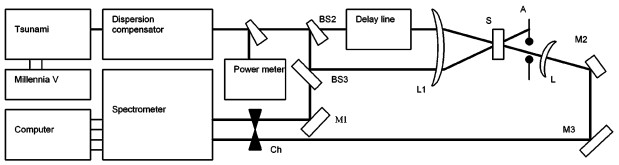

Fig. 2 Experimental setup used for spectrally resolved two-beam coupling measurements of non-linear optical susceptibility. M are mirrors, BS are beam splitters, S is the test sample, A is a slit, L are lenses, Ch is a two-channel stroboscopic interrupter. Millennia V is a pump laser for femtosecond generator Tsunami. The Tsunami generates 35 fs laser pulses with a mean energy per pulse of 1–3 nJ. The pulse repetition rate is 80 MHz. The central wavelength is 795–800 nm.

Laboratory, UK, operating under beam conditions of 2 GeV, 200 mA using a Si (111) monochromator.

Appropriate amounts of copolymer samples were finely ground with boron nitride and pressed (5 bar) into 13 mm pellets producing a suitable edge jump between 0.2 and 1. The samples were cooled to 80 K in a cold finger liquid nitrogen cryostat. Spectra were recorded in transmission mode. EXAFS data were collected with 60% harmonic reduction up to k = 16 Å^{-1}. The typical acquisition time for each dataset was 1 h, and typically three datasets were collected and averaged for each sample. Bis(benzene)chromium, Cr_2O_3, and 5 μm Cr foil were used as structural and oxidation state standards. Exact calibration of the X-ray energy for accurate measurement of small shifts in the XANES features was achieved by simultaneously recording the spectrum of a suitable reference sample in the monitor position.

Data reduction and analysis of the X-ray absorption spectra was performed using the programs EXBACK and EXCURV98.[6] EXAFS structural refinements were carried out using k^3 weighting.

Z-scan third order optical susceptibility measurements

Two independent series of experiments were performed using picosecond pulses from a Nd:YAG laser (at wavelength λ = 1064 nm) and a Nd^{3+}-doped phosphate glass laser (at wavelength λ = 1054 nm). In the first series the Nd:YAG laser with passive mode-locking was used as a master laser. A polymer Q-switcher was the passive mode-locker. The Q-switch polymer film was based on polymethyne dyes incorporated in a matrix.[7] The laser generated a pulse train (20–30 pulses) with each pulse duration of $\tau \sim$ 40 ps, repetition rate 18 ns, and pulse energy about 10^{-6} J. In the second series, a Nd^{3+}-doped phosphate glass master laser with a passive Q-switcher was used. The duration of each pulse in the train was *ca.* 3–4 ps. Only one picosecond pulse from each train was used for the non-linear optical measurements. A Pockels cell was placed between two cross polarizers for pulse selection. Electric pulses, which opened the polarization shutter, were synchronized with the largest optical pulse in the train.

The selected picosecond pulse was amplified in a double-pass amplifier (based on Nd:YAG crystal or Nd:phosphate glass) with a polarization isolator. This amplifier increased the pulse energy up to 10–50 μJ (controlled by a photodetector PD 1, Fig. 1).

The light beam was then focused by a lens of focal length F = 12 cm onto the polymer under study (a film or solution layer). Once the beam had passed through the sample we measured the intensity in the centre of the beam in the far wave zone (with photodetector PD 3) and total power (with wide-aperture photodetector PD 2).

Spectrally resolved two-beam coupling measurements of non-linear optical susceptibility

We used the method reported originally[8] with our modifications,[9] the experimental setup being easy to align and for fine adjustment (Fig. 2). The samples were prepared by sandwiching a layer of composite material (thickness 50 μm) between glass slides.

Electro-optical measurements

Measurement of the electro-optical coefficient r_{13} of polymer composites based on CrPAN and CrMePAN with T_g close to room temperature (thickness *ca.* 50–100 μm) has been performed using an interferometer technique efficient in the measurement of refractive index changes.[10,11] This method (Fig. 3) has been used to study the excited states of pumped Nd:YAG crystals,[12] small absorptions in optical materials in the middle infrared frequency band,[13,14] and the measurement of heavy metal concentrations in water.[15,16]

The polymer films were gripped between two glass-plates coated with a tin oxide electrically-conducting layer. Each conducting layer was divided into two electrodes by a vertical

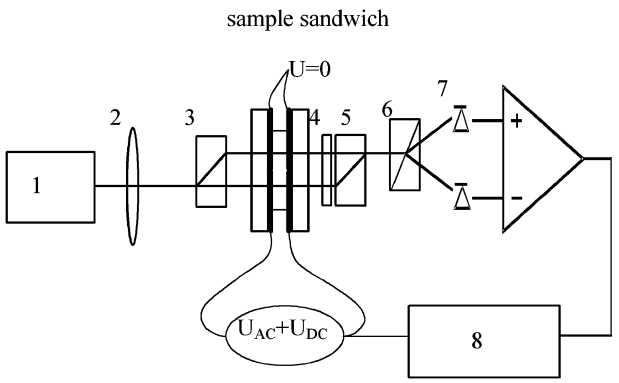

Fig. 3 Schematic diagram of experimental setup. 1 is diode laser at λ = 0.65 μm, 2 is collimating lens, 3, 5 are beam displacing prisms, 4 is 90° polarization rotator, 6 is Wollastone prism, 7 are photodiodes, 8 is lock-in amplifier EG&G 5208.

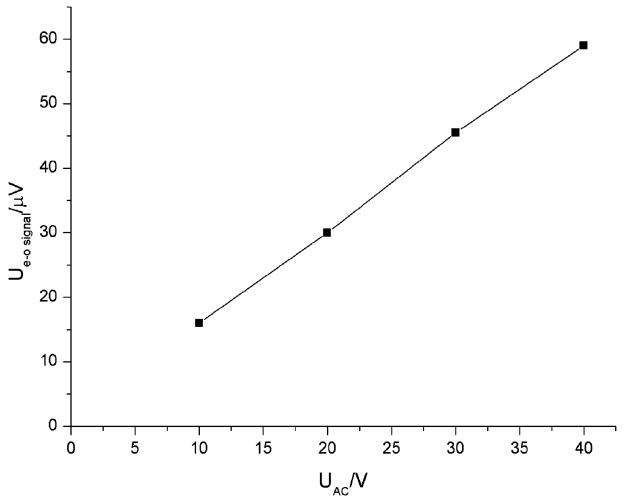

Fig. 4 Electro-optical response of sample *I vs.* AC voltage.

groove. To one pair of electrodes were applied both direct and alternating voltages, whilst the other two were shorted out. The sandwich was placed in a Jamen-Lebedev interferometer at right angles to the laser beams in such a way that one beam passed the film in the biased part of the sample while the second beam tested the polymer without applied voltage. The electro-optical phase difference was detected with a lock-in amplifier at the frequency of the AC voltage. The measured phase difference depends on U_{AC} as a linear function (see Fig. 4).

The applied AC voltage changes the relative phase φ_1–φ_2 between the arms of the interferometer. The resulting modulation of the light intensity on the output of channels I and II of the interferometer is given by

$$I_I = \tfrac{1}{2}\left(I_1 + I_2 + 2\sqrt{I_1 I_2}\cos(\varphi_1 - \varphi_2)\right)$$

$$I_{II} = \tfrac{1}{2}\left(I_1 + I_2 - 2\sqrt{I_1 I_2}\cos(\varphi_1 - \varphi_2)\right).$$

$$\varphi_1 - \varphi_2 = \varphi_0 + A\cos(\Omega t)$$

where φ_0 is the constant phase difference without electro-optical modulation. For achievement of maximum sensitivity it must be shifted to zero by alignment of the arm lengths of the interferometer.

A is the modulation amplitude due to the electro-optic effect given by

$$A = 2\pi\Delta nd/\lambda = \pi r_{13} n^3 V_{AC}/\lambda.$$

where V_{AC} is the amplitude of the applied AC voltage.

For a small modulation amplitude and $\varphi_0 = 0$ the voltage of the electro-optical signal V_{signal} at the output of the operational amplifier is proportional to

$$V_{signal} \propto 2\sqrt{I_1 I_2}\pi r_{13} n^3 V_{AC}\cos(\Omega t)/\lambda.$$

The product $\sqrt{I_1 I_2}$ can be determined independently by measuring variations in the DC voltage at the output of the operational amplifier *versus* φ_0. Maximum V_+ and minimum V_- DC voltages are related to the product $\sqrt{I_1 I_2}$ by

$$\sqrt{I_1 I_2} = V_+ - V_-/2$$

To summarize, the electro-optical coefficient may be written by

$$r_{13} = \frac{\lambda}{\pi n^3 V_{AC}} \frac{V_s}{V_+ - V_-},$$

where V_s is the amplitude of the electro-optical signal detected by a lock-in amplifier at the frequency of the AC voltage.

Results and discussion

Synthesis of polymeric nanocomposite precursors and their spectral properties

The polymeric nanocomposite precursors were prepared by the reaction of $(Cr(Et_nC_6H_{6-n})_2$ (n = 1,2,3) with CN-containing vinyl monomers (acrylonitrile, crotonitrile or ethyl 2-cyanopropenoate) under argon. The molar ratio Cr : monomer was varied from 1 : 4 to 1 : 20. The process is initiated by electron acceptors such as oxygen, fullerene-60, TCNE or TCNQ and is accompanied by polymerization of the monomer with up to 90–100% conversion. The reaction takes place in the presence of radical traps such as 1,3-di-*tert*-butyl-*o*-benzoquinone, so a radical mechanism of polymerization can be ruled out. The presence of CN groups in the monomer molecules evidently plays an important rôle in this reaction since common vinyl monomers such as styrene, α-methylstyrene, methylmethacrylate and vinyl chloride are unreactive towards bis-arene metal complexes.

In all the cases, the reaction results in the formation of a homogeneous oligomeric product readily soluble in acetonitrile, DMF or DMSO, and containing *ca.* 8 monomer units as determined by elemental analysis. The oligomers being insoluble in THF we have been unable to determine the molecular weights with our SEC columns. The molecular weights are too low for the light scattering technique of molecular weight determination to be successful, and methods making use of colligative properties (*e.g.* VPO or freezing-point depression) are unsuitable since they are greatly influenced by the presence of small molecules.

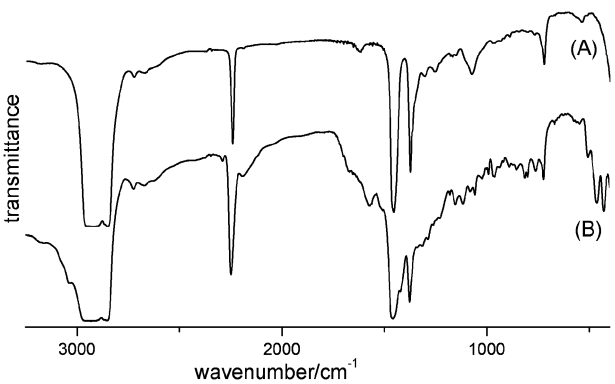

Fig. 5 IR spectra of Nujol mulls of PAN (A) and CrPAN (B).

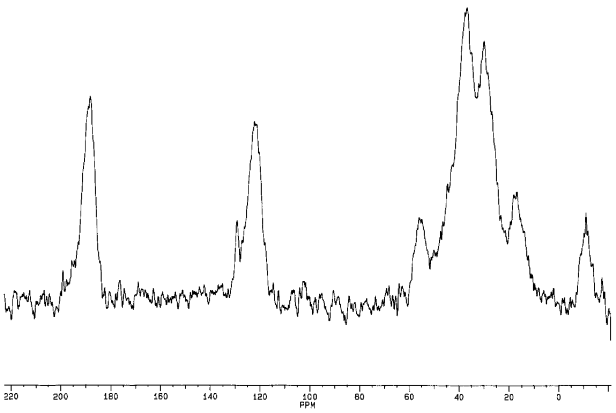

Fig. 6 Solid state ^{13}C NMR spectrum of CrPAN.

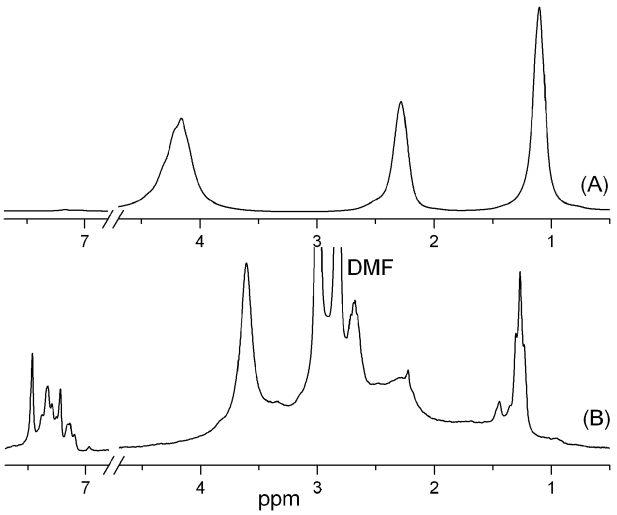

Fig. 7 ^{1}H NMR spectra of Ar_2Cr (A) and CrPAN (B) in DMF-D7 solution.

The IR spectra of the products based on acrylonitrile (CrPAN) and crotononitrile (CrPMeCN) contain all the bands characteristic of the corresponding polymers[17] (Fig. 5).

Similarly, the solid state ^{13} NMR spectrum shows signals at 28.5 and 37.3 ppm corresponding to the methylene and methyne carbon atoms of PAN and a resonance at 121.8 ppm for the CN carbon (Fig. 6).[18] There is also evidence of the persistence of the sandwich structure in all the polymers, the IR bands in the region 425–475 cm^{-1} being characteristic of a metal–arene bond.[19] Moreover, the ^{13}C NMR resonances at 187.8 ppm can be unequivocally attributed to the coordinated aromatic sandwich carbons shifted with respect to the signal for the free aromatic ligands.[19] The ^{13}C NMR resonances at 14–17 ppm are assigned to the methyl carbons in the aromatic ring ethyl substituent. EXAFS analysis confirms that the chromium is present only in the form of the bis-arene complex.

However, there is evidence for a very significant influence of the polymer matrix on the metal complex, a comparison of the ^{1}H NMR spectra for CrPAN and $(arene)_2Cr$ showing a very large shift to low field for the resonances of the aromatic protons (from 4.16 ppm to 7.1–7.5 ppm) (Fig. 7). The resonances are broad, consistent with the polymeric nature of the product and also with the fact that a mixture of isomers was used.

Additionally, the initial ratio of aromatic/methyl protons in the sandwich complex decreases as the reactions with acrylonitrile and crotononitrile proceed (Table 2), consistent with the occurrence of the cyanoethylation reaction giving a direct bond between the arene and the polymer chain. This is confirmed by the signal at 55.7 ppm in the solid-state ^{13}C NMR spectrum of CrPAN (Fig. 6), absent in the spectra of both the pure complex and polyacrylonitrile, and which can be assigned to the acrylonitrile CH_2 groups covalently bonded to the arene ligand. Further evidence for the formation of a bond between the arene ligand and the polymer chain is provided by the ^{1}H NMR spectrum of CrPAN prepared from bis(benzene)chromium (Fig. 1S†) showing a complicated structure for the aromatic proton resonances instead of a singlet for benzene if there were no substitution reaction.

The results obtained for acrylonitrile and crotononitrile confirm the mechanism we suggested previously of aromatic ring cyanoethylation followed by polymerization.[4] Thus, the signal at 55.7 ppm in the solid-state ^{13}C NMR spectrum of CrPAN, which is absent in the spectra of both the pure complex and polyacrylonitrile, can be assigned to the acrylonitrile CH_2 groups covalently bonded to the arene ligand.

In view of the fact that a free radical mechanism can be ruled out (*vide supra*), we suggest the reaction is initiated by a charge transfer complex formed between an electron acceptor with the chromium atom followed by a reversible one-electron transfer polymerization mechanism resulting in cyanoethylation of the arene ligand. Chain propagation also occurs by the same mechanism (Scheme 1). This mechanism seems quite reasonable providing an initiation centre close to the propagation centre. Thus, star-shaped molecules consisting of a central bis-arene chromium species with polyacrylonitrile arms

Table 2 Composition of $(Et_nC_6H_{6-n})_2Cr$ (n = 1,2,3) before and after reaction with 8 equiv. $RCH_2{=}CHCN$ (R = H, CH_3)

	Ratio of aromatic protons to CH_3 in Cr complex			Average no. of aromatic protons per Cr atom		
	Initially, determined by					
Monomer	^{1}H NMR	GLC	In product of reaction (^{1}H NMR)	Initially	In product of reaction	Average no. of reacting aromatic protons per Cr atom
$CH_2{=}CHCN$	0.93[a]	0.92	0.67	8.5	6.7	1.8
$CH_3CH{=}CHCN$	0.93[b]	0.94	0.50	8.8	4.1	4.7

[a] Sample (1). [b] Sample (2).

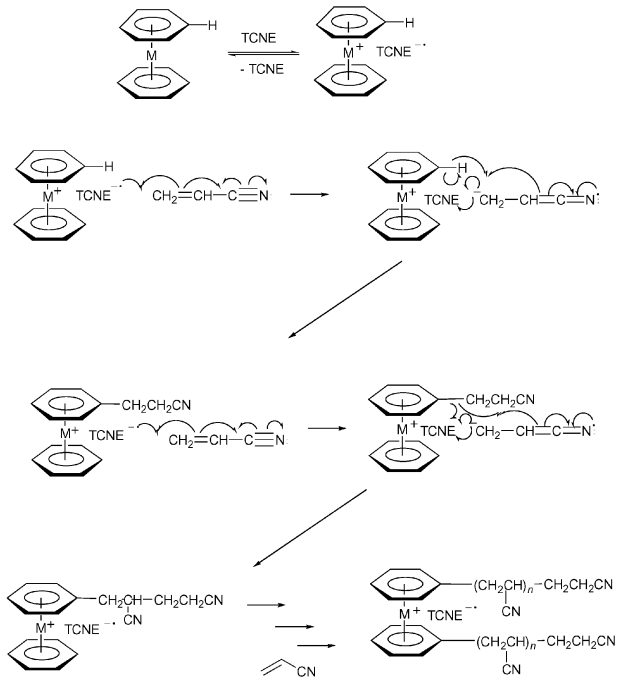

Scheme 1 Suggested polymerization mechanism.

covalently bonded to the arene ligands are formed as a result of the reaction.

Interestingly, the degree of aromatic hydrogen atom replacement in the arene ligand is noticeably greater for crotonitrile than for acrylonitrile. We explain this by a different ratio of monomer cyanoethylation and polymerization rates. Indeed, if the propagation is significantly faster than cyanoethylation the probability of replacement becomes rather low. Thus, crotonitrile, which is polymerized more slowly in the presence of anionic species because of the inductive influence of the CH_3 groups, is more efficient as a polycyanoethylation agent than is acrylonitrile.

Also, it has been established that ethyl 2-cyanopropenoate (ECA) is polymerized almost immediately under the reaction conditions forming a polymeric phase separated from the chromium complexes. Nevertheless, the heterogeneous reaction mixture gives homogeneous solutions in acetonitrile and DMF. After solvent removal, a homogeneous product is obtained. The ^{1}H NMR spectrum of this product shows no signal at 7.2 ppm corresponding to the aromatic protons of the cyanoethylatated ligands in the sandwich structures. At the same time, we observed a strong asymmetrical extension of the ECA group ethylene proton resonance at 4.3 ppm because of superposition with the free chromium complex aromatic proton signal at 4.16 ppm making it impossible to calculate the ratio of aromatic to CH_3 protons in the Cr complex. But it is reasonable to suppose that polymerization of ECA in the presence of the sandwich proceeds without cyanoethylation of the arene ligands. The chromium complex forms a homogeneous solution in poly(ethyl 2-cyanopropenoate) (PECA) because of coordination of the ester C=O group to the central metal atom. The IR spectrum of CrPECA provides direct confirmation of this showing two very strong C=O bands at 1750 cm^{-1} and 1608 cm^{-1} (Fig. 2S†), the band at lower energy corresponding to the C=O groups coordinated to chromium. Coordination also results in substantial broadening of all the signals in the ^{1}H NMR spectrum of CrPECA with respect to pure PECA (Fig. 8).

The preparation of non-linear optical compositions based on the (arene)$_2$chromium-containing polymeric nanocomposite precursors

The ability to form good optical-quality films cast from acetonitrile solutions is a very important and valuable property of the polymeric nanocomposite precursors obtained by the above method. During the film formation bis-(arene)chromium(0) is oxidized by air oxygen giving very stable (arene)$_2$-Cr^+^{1}OH species incorporated into an optically-transparent polymer matrix. The films undergo a colour change from red-brown to yellow depending on the complex concentration and the nature of the monomer. It is very important to note that the process of film formation also involves the hydrolysis of polyacrylonitrile by the strongly alkaline $[Cr(arene)_2]^+OH^-$ species. It is well known that alkaline agents cause the cyclization of acrylonitrile C≡N groups giving ladder-structured polynaphthyridine-type polymers with conjugated C=N bonds.[20–25] The simplified scheme for this process for CrPAN is illustrated in Scheme 2, and the molecular model of a sandwich structure covalently bonded with one branch of hydrolyzed polyacrylonitrile is shown in Fig. 9. The presence of conjugated structures in oxidized CrPAN is confirmed by solid state ^{15}N NMR, IR, UV and fluorescence spectroscopies. In the solid state ^{15}N NMR spectrum, in addition to the resonance at 132.0 ppm typical for the nitrile group, signals at 115.8 and 99.0 ppm are observed. These resonances are shifted to lower field as a result of lengthening of the C≡N bond and reduction in its multiplicity. The absorption and fluorescence spectra in the region 300–500 nm are very typical for hydrolyzed PAN but not for pure (arene)$_2$$Cr^+OH^-$ and unhydrolyzed PAN the latter being completely transparent in the visible region.

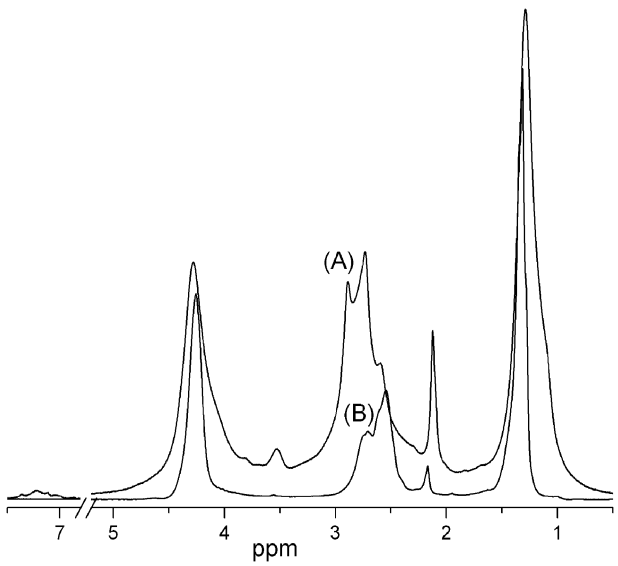

Fig. 8 ^{1}H NMR spectra of CrPECA (A) and PECA (B) in DMF-D7 solution.

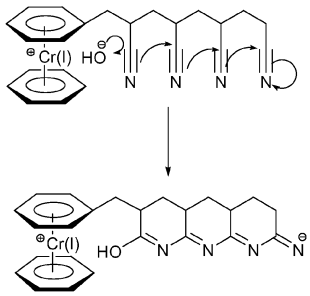

Scheme 2 The formation of CN-conjugated ladder-structured polynaphthyridine-type polymers for CrPAN.

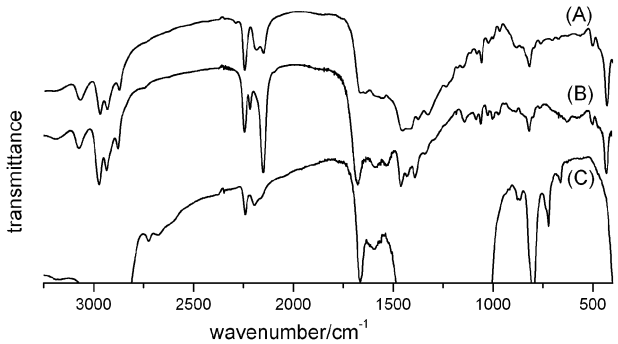

Fig. 10 IR spectra of CrPAN (A) and CrMePAN (B) films, and Nujol mull of alkali-hydrolyzed PAN (C).

A comparison of the IR spectra of pure PAN after alkaline hydrolysis (prepared according to the described method[24]), CrPAN and CrPMePAN films (Fig. 10 (A), (B), and (C)) shows that:

(i) Cyclization of the CN groups with $(arene)_2Cr^+OH^-$ species as well as with alkali results in the appearance of intense IR bands in the region 1580–1670 cm^{-1} corresponding to various forms of cyclic C=N conjugated ladder structures.[21]

(ii) The additional absorption bands for the CN groups at 2200 cm^{-1} and 2150 cm^{-1} are shifted to lower energy with respect to initial (not hydrolyzed) PAN, and the CrPAN band at 2245 cm^{-1} (Fig. 5) appears in all the spectra after hydrolysis resulting in cyclization has occurred. In accordance with the literature[21] the lower frequency bands result from CN groups forming part of a conjugated system. However, in bis-(arene)-chromium(+1)-containing polymers these bands are much more distinct and intense. In particular, the band at 2150 cm^{-1} is observed only as a slight shoulder in hydrolyzed PAN whereas in CrPMePAN it is much more intense than the CN band at 2245 cm^{-1}. This observation suggests there is some coordination between the CN groups in the polyacrylonitrile arms and chromium(+1) in the sandwich structure. In accordance with the data of Miller and Epstein for charge-transfer vanadium and manganese sandwich complexes with TCNE the lower energy CN absorption is assigned to interaction of the metal with CN groups.[26] With an increasing number of M → NC interactions the $\nu_{C\equiv N}$ absorptions shift to lower energy and the highest energy absorption is attributed to CN groups not bonded to the metal. This is in good agreement with our observation (Table 2) that the aromatic ligands in CrPMePAN undergo a higher degree of polycyanoethylation than those in CrPAN and thus the central chromium atom is surrounded by a larger number of CN-containing branches covalently bonded with the arene ligands.

The presence of CN conjugated systems is also supported by the UV/visible and fluorescence spectra of hydrolyzed Cr^+PAN (Fig. 11). The absorption spectrum consists of two bands with maxima at 283 nm and 343 nm reflecting MLCT and LMCT transitions, respectively,[27] in chromium bis-arene complexes. A smooth decline in the long-wavelength part of the absorption spectrum should also be noted. Under excitation into this part of the absorption spectrum (λ_{exc} = 370 nm) a broad fluorescence band with maxima at 463 and 505 nm is registered. It is very different from the fluorescence excitation spectrum of free $(arene)Cr^+OH^-$ which reflects only the benzene ring absorption spectrum perturbed by the interaction with the Cr^+ ion (Fig. 12). As the excitation wavelength is tuned from 360 to 430 nm, the fluorescence spectrum shifts towards the red and is gradually transformed into a single band at 505 nm. This provides evidence for the presence in the solution of two types of polynaphthyridine chains with different lengths of the π-conjugation system. This is also shown by the dependence of the position of the long-wavelength

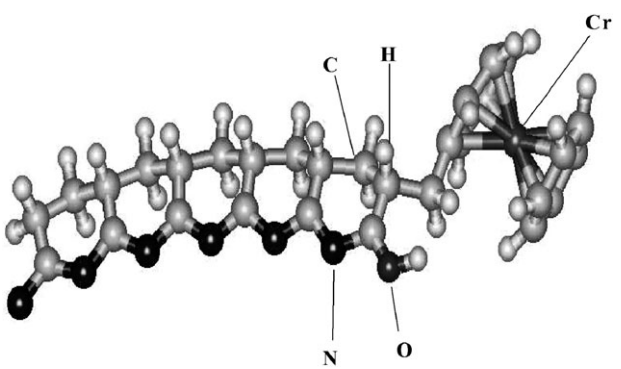

Fig. 9 Molecular model of a CrPAN sandwich structure covalently-bonded with polynaphthyridine chain.

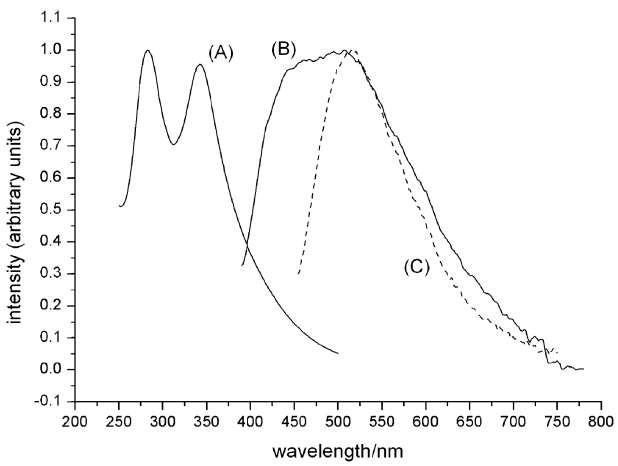

Fig. 11 Absorption (A) and fluorescence (λ_{exc} = 370 nm, (B); λ_{exc} = 435 nm, (C)) spectra of Cr^+PAN.

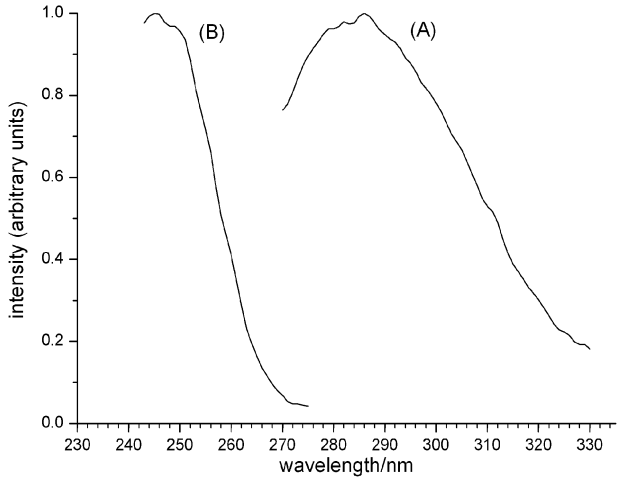

Fig. 12 Fluorescence (λ_{exc} = 255 nm) (A) and fluorescence excitation (λ_{reg} = 310 nm) (B) spectra of $Cr^+(C_6H_6)_2$.

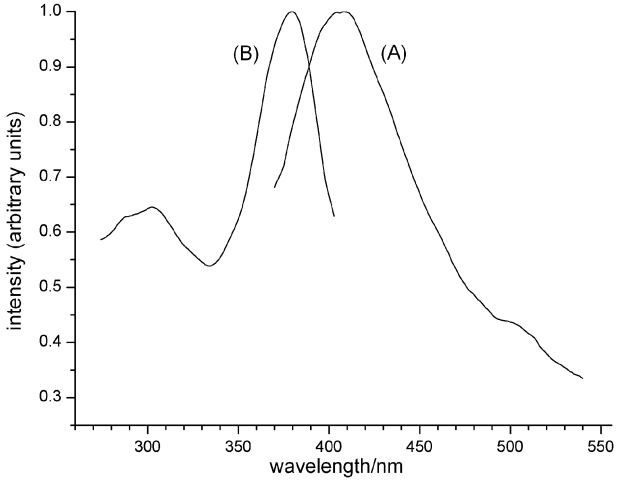

Fig. 13 Fluorescence (λ_{exc} = 340 nm) (A) and fluorescence excitation (λ_{reg} = 430 nm) (B) spectra of PAN.

maximum of the fluorescence excitation spectrum on the registration wavelength. It can be seen that the fluorescence spectrum at 468 nm is formed by two types of centres having fluorescence excitation spectra with maxima at 378 nm and 430 nm, respectively. The comparison of the spectroscopic characteristics of free PAN after alkaline hydrolysis (Fig. 13) and that of Cr^+PAN shows a significant increase of the Stokes shift which reaches 4800 cm^{-1} for Cr^+PAN and only 2000 cm^{-1} for free PAN. This demonstrates the presence of intramolecular charge separation in the first excited state of the conjugated system in Cr^+PAN, which, in turn, should give rise to higher $\chi^{(3)}$ values for this compound. It can also be an additional indirect piece of evidence for the fact that CN conjugated chains exist in Cr^+PAN not independently but covalently bonded with the sandwich structure. It is very interesting that analogous investigations of hydrolyzed free PECA and Cr^+PECA did not reveal significant changes in the spectral characteristics nor an increase in the Stokes shift in the presence of the bis(arene) complex. In the light of the aforesaid it also implies an absence of any covalent bond between PECA and the arene ligand. Finally, the absence of any significant intramolecular charge redistribution in Cr^+PECA allows one to expect lower $\chi^{(3)}$ values.

The oxidation of the polymeric nanocomposite precursor Cr(0)PAN occurs with TCNE as oxidizing agent (equimolar ratio of bis(arene)$_2$ Cr and TCNE) in acetonitrile under anaerobic conditions. The very intense bright-red colour of the solution is the result of charge-transfer complex formation. The presence of a charge-transfer complex is confirmed by the appearance of the absorption band at 540 nm in the visible spectrum of the resulting product (Fig. 14).

The EPR spectrum of an acetonitrile solution of the charge-transfer complex revealed a signal typical of Cr(+1) in the bis-arene complex with g = 1.987 (Fig. 15 (A)).[26,28] At low temperatures (230 K) the hyperfine structure of the EPR signal can be observed. The very similar values of the superfine coupling constants, a_1 = 3.5 G and a_2 = 3.6 G, indicate the superposition of the signals corresponding to bis(arene)Cr^+ species with even and odd numbers of aromatic protons in the aromatic rings. This was confirmed by the result of a signal simulation (Fig. 15 (B)), the best fit for the simulated signal to the experimental signal being obtained with the assumption of the concomitant presence of a Cr(+1) paramagnetic species without resolution in addition to the signals corresponding to bis(arene)Cr^+ species with even and odd numbers of aromatic protons in the aromatic rings. Indeed, it is known that bis(arene) complexes with bulky (or numerous) ring substitutents exhibit hyperfine line broadening because of hindered molecular rotation, and no hyperfine structure is observed.[28] Thus, a possible rationalization for the presense of Cr(+1) paramagnetic species giving broadened hyperfine lines even at low temperatures is the presence of bulky polymeric substituents in the benzene rings. It is interesting that the TCNE radical-anion signal is absent in the spectrum unlike for free (arene)$_2Cr^+$ as described in the literature.[29] This can be explained by the involvement of the TCNE radical-anion electrons in the CN conjugated structure formed as a result

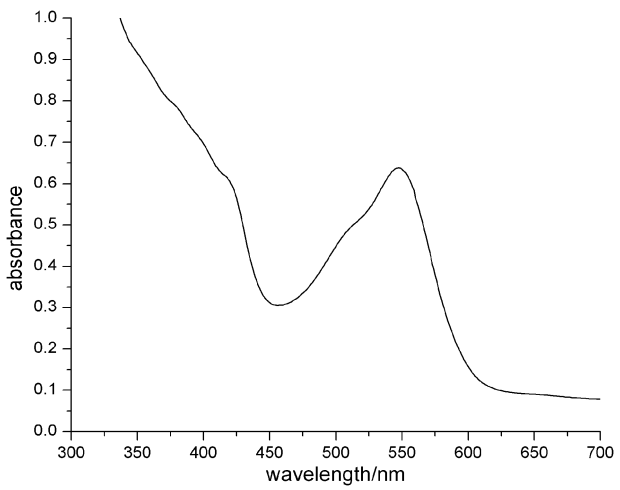

Fig. 14 UV/Vis spectrum of CrPAN.TCNE charge-transfer complex in acetonitrile.

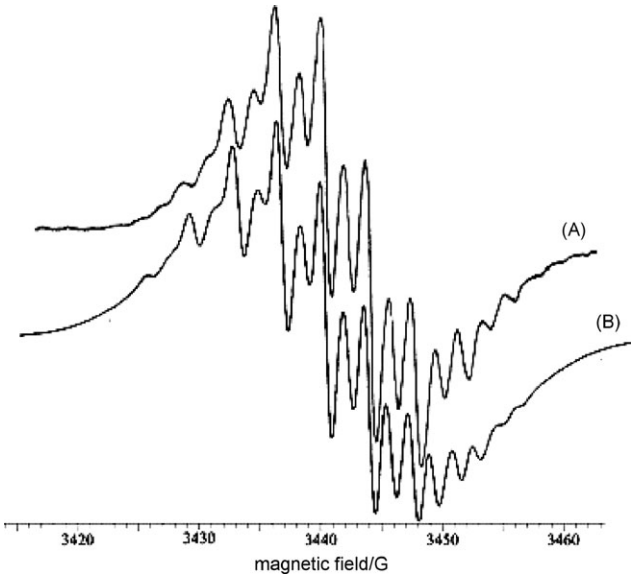

Fig. 15 EPR spectrum of the charge-transfer complex of CrPAN with TCNE in acetonitrile solution at 230 K; experimental (A), simulated (B).

of anionic cyclization of the PAN units. Thus, one can expect a high electronic polarizability resulting from charge-transfer from bis(arene)species to large ''diffuse'' anions with extended π-conjugation systems.

A very important aspect in the investigation of non-linear optical polymers is the preparation of materials of high optical and mechanical quality. To that purpose in some cases we used a polycyanoacrylate (PECA) transparent matrix which is completely compatible with all the polymers we obtained. Also we used small additions of malonodinitrile as plasticizer in order to avoid cracking and for control of the glass-transition temperature.

TEM micrographs of the films prepared from hydrolyzed CrPAN and the charge-transfer complex $Cr^{+}PAN\text{-}TCNE^{-}$ in a PECA matrix (1 : 10) show the presence of nanostructures of mainly elongated shape (Fig. 16). The electron diffraction pattern (inset Fig. 16a) shows the presence of some crystallographic order consistent with the formation of self-organized structures.

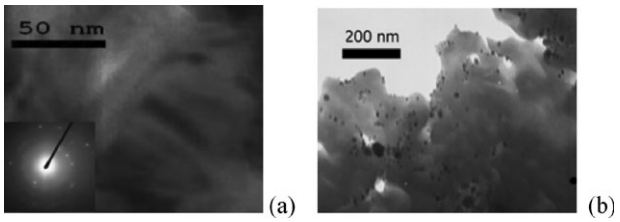

Fig. 16 TEM micrographs of the films prepared from hydrolyzed CrPAN (a) and the charge-transfer complex $Cr^{+}PAN\text{-}TCNE^{-}$ in PECA matrix (1 : 10) (b).

X-Ray absorption spectroscopy (EXAFS, XANES)

Detailed characterisation of the structure and bonding of these novel polymeric materials is essential to understanding and applying their properties. Extended X-ray absorption fine-structure spectroscopy (EXAFS)[30] involves incident X-rays ejecting core electrons from the atom under study (*e.g.* a 1s (K) electron from a Cr atom). This photoelectron is backscattered by the neighbouring atoms and the resultant spectrum gives information about the local co-ordination environment of the central atom, including bond lengths and co-ordination numbers. This is a short range effect (up to 6 Å). It is ideal for samples lacking long-range crystalline order. For X-ray absorption near-edge spectroscopy (XANES) the photoelectron is not completely ionised but promoted to an empty higher level orbital. This provides direct information on the oxidation state and bonding environment of the central atom.[30,31] X-Ray absorption spectroscopy is rarely employed in the analysis of polymers, primarily because the majority of polymers are carbon-based and the necessary X-ray energies are not easily accessible. However it can give valuable information on the structure and bonding of polymers containing inorganic elements such as metal atoms.[32]

X-Ray absorption spectra at the Cr K edge were obtained for samples of CrPAN, $[CrPAN]^{+}TCNE^{-}$, and $[CrPAN]^{+}OH^{-}$. and initial data analysis has been undertaken. The XANES shows that in all these materials the chromium atoms are in low oxidation states. In CrPAN and $[CrPAN]^{+}TCNE^{-}$, a single Cr–C distance was found in the EXAFS data refinement, showing that the arene rings are parallel and symmetric as in bis(benzene)chromium. The Cr–C distances in these two materials are very similar to the 2.13 Å in bis(benzene)chromium. In the hydroxide derivative $[CrPAN]^{+}OH^{-}$, more than one metal –carbon distance was resolved, showing either that the two arene rings are at different distances from the metal, or that they are tilted rather than parallel. Another distance was also resolved, which is interpreted as Cr–O, showing direct coordination of the hydroxide ion to the chromium atom. No significant change was observed in the Cr–C distance on oxidation of CrPAN to form $[CrPAN]^{+}TCNE^{-}$, and the XANES of these two complexes are also very similar. This is surprising, because it had been expected that oxidation would remove an electron from a Cr-arene bonding molecular orbital. Possibly the HOMO in CrPAN is associated with the polyacrylonitrile parts of the structure. If this is the case, it would have important implications for the polarisability behaviour. Further refinement of the EXAFS data is under way, and correlation of the results with the non-linear optical properties of these materials is in progress.

Electro-optical coefficient measurements

Two polymer composites were tested, composite **I** containing hydrolyzed CrPAN (95 wt.%) and malonodinitrile as plasticizer (5 wt.%) and composite **II** containing 100% hydrolyzed CrMePAN, the molar ratio Cr : monomer being 8 in each composite. The dependence of the electro-optical coefficient $r_{33}n^3$ on poling DC voltage for films of composites **I** and **II** is shown in Fig. 17. A very high electro-optical response is found for CrMePAN (much less for CrPAN) at a relatively low DC voltage. The dependence of the electro-optical coefficient $r_{33}n^3$ on U_{AC} frequency is shown in Fig. 18. We observed a

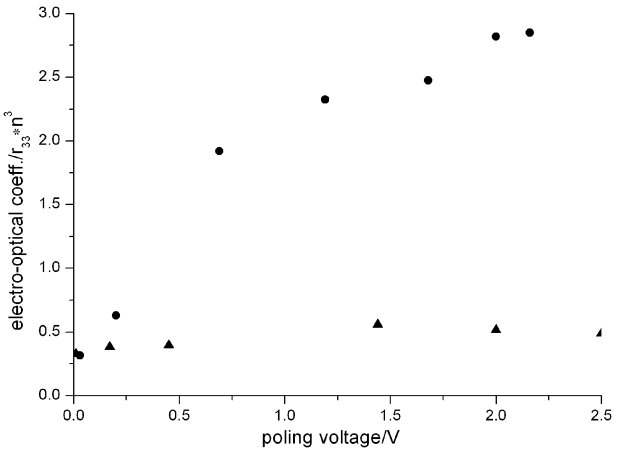

Fig. 17 Dependence of electro-optical coefficient $r_{33}n^3$ on poling DC voltage for films of composite **I** (▲) and composite **II** (●) tested at 29 °C.

significant enhancement of the signals with a decrease in the modulation frequency. Thus, an essential contribution of orientation effects to the electro-optical response can be noted. The highest value of the electro-optical coefficient ($r_{33}n^3$) was obtained for composite **II** at the lowest modulation frequency available to us (210 Hz) and with a poling DC voltage 2.16 V, corresponding to 4.245 pm V^{-1}.

It is very interesting that an electro-optical response was obtained in the absence of almost any applied bias voltage (Fig. 17). This may be the result of the presence of some anisotropy in the internal structure of the studied polymers as confirmed by the results of electron diffraction studies (Fig. 16 (a) insert) indicating the presence of self-organized structures.

$\chi^{(3)}$ Non-linear optical properties

Three polymer composites were tested; composite **I**, composite **III** containing hydrolyzed CrPAN in a PECA matrix (weight ratio 1 : 3), composite **IV** containing the charge-transfer complex Cr^+PAN-$TCNE^-$ in a PECA matrix (weight ratio 1 : 10). Malonodinitrile was used as plasticizer (5 wt.%) in all three composites.

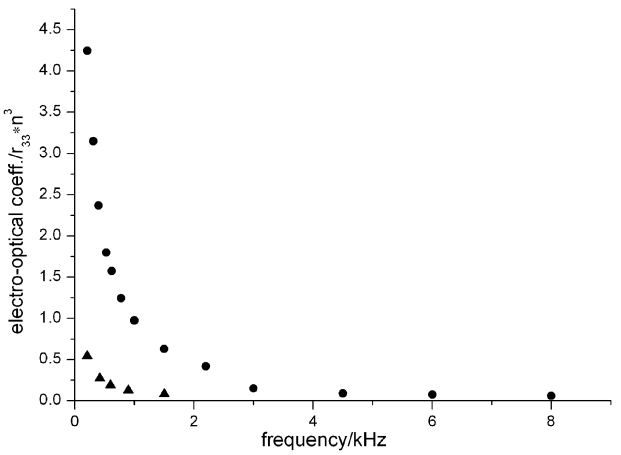

Fig. 18 Dependence of electro-optical coefficient $r_{33}n^3$ on U_{AC} frequency for composite **I** (▲) and composite **II** (●).

The Z-scan method is used in investigations of non-linear polymers. As is well known, this method is based on the influence of the non-linear lens (induced by an optical beam inside the thin non-linear layer) on the beam size in the far field outside the non-linear layer.[33] The theory of wave self-focussing is the basis for the description of the Z-scan method. The following expression can be theoretically found in the approximation of the small non-linear non-inert variation of refractive index.[33]

$$\Delta T \cong 0.4\ \Phi_{nl} = 0.4\ kn_2\ Il,$$

where ΔT the difference between the values of the transmission coefficients (ratio between the beam power passed through a small aperture on the beam axis and the total beam power passed through the non-linear layer) in the extremum points of the Z-scan curve, Φ_{nl} is the non-linear phase addition along the beam axis, n_2 is the third-order non-linear optical refractive index, I is the light beam intensity along the beam axis, k is wave number, and l is the thickness of the non-linear media. Knowing the intensity along the beam axis and the value of ΔT measured by experiment, the value of the non-linear refractive index n_2 can be found.

In our Z-scan experiments the registering photodetector (PD 3 in Fig. 1) was placed 50 cm away from the sample under study. It received part of the beam with a diameter of 1 mm in the near-axis area. The total diameter of the beam on the photodetector was ~10 mm. The relation between the registered part of the beam and its total size, the S parameter,[34] was large enough for stable detection of the signal, corresponding to near-axis power. On the other hand, the S parameter was small enough to obtain the Z-scan dependence but large enough to decrease the spatial fluctuations of the optical beam intensity because of random inhomogeneities of the optical scheme.

An additional registration of the total beam power passed through the nonlinear layer (with a wide-aperture photodetector PD 2) allowed us to detect linear and non-linear absorptions in the sample. The measurements of sample transmission dependence in the total aperture with a pulse energy of ~10–20 μJ showed the absorption of CrPAN polymer films, ~10–30 cm^{-1} corresponding by its order of magnitude with linear absorption of the polymers when the resonant transition was far from the measurement area in the spectra. Measurements of the dependence of sample transmission into the total aperture on the sample coordinate along the focal waist confirmed the absence of two-photon absorption at the wavelengths (1054 nm and 1064 nm) and beam intensities used. The typical dependence of sample transmission in full aperture was not observed in our Z-scan measurements. So the non-linear absorption coefficients for the studied polymers were less than 2 cm MW^{-1}.[35] This result is in good agreement with the measured absorption spectra of the polymers.

The absence of large linear absorption and resonant two-photon absorption was also confirmed in the measurement of the absorption spectra (Fig. 19). The upper limit of the strong absorption band for CrPAN lies at wavelength 400–450 nm.

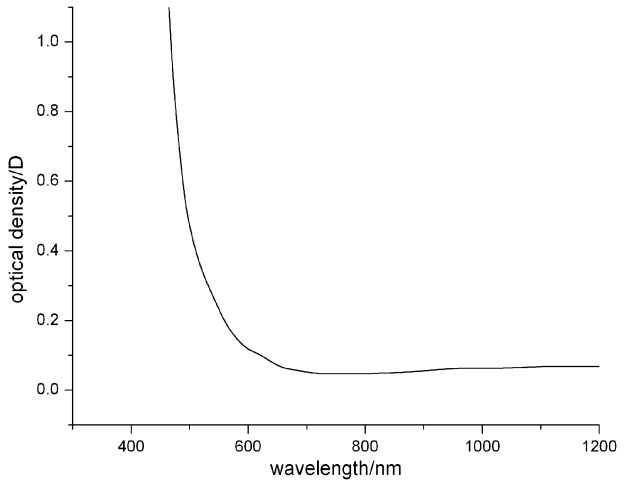

Fig. 19 Absorption spectrum for the bis(arene)chromium-containing polyacrylonitrile film.

To calibrate the Z-scan setup and test the method a cell with chloroform was used (layer thickness 2 mm). The value of the non-linear refractive index of chloroform is well known ($n_2 = 5 \times 10^{-15}$ cm^2 W^{-1})[36] and has the sign of focussing non-linearity. The value of the non-linear refractive index determined its major contribution to the total non-linear wave phase incursion after passing through the cell as compared to the contribution of the glass walls (typical values of the non-linear refractive index for optical glasses are 4–14 $\times 10^{-16}$ cm^2 W^{-1}).[34] Our measurements with laser pulses of energy 20 μJ showed, indeed, focussing non-linearity in chloroform. Within experimental error (*ca.* 20%) the calibration value of n_2 for chloroform was 5×10^{-15} cm^2 W^{-1}, the same as the literature value.[36]

To determine the applicability of the approximation of small non-linear perturbation, by which the expression for the Z-scan was obtained (expression (1) below), additional experiments were made with different energies of test pulses (10–50 μJ). These Z-scan measurements (power recorded with photodetector PD 3 at various positions of the cell in the focus area) allowed us to determine the non-linear refractive indices of the polymer films of interest. The measured dependence of the near-axis power on the sample coordinate agrees well with the theoretical curves, described by expression (1) below with different values of the non-linearity coefficient n_2. The values of the third-order optical susceptibility for the studied polymers were calculated based on the results of experiments with the linearly polarized test beam (see Table 3).

In our measurements the durations of the test laser beams were 40 or 3 ps, being less than the typical time of thermalization of polymer excitation (electron-oscillation relaxation in the films) of about several tens of picoseconds.[37] So, the transformation of absorbed energy into heat energy was complete only at the end of the optical pulse. Moreover, the time of sound wave propagation in the polymer film (thickness 40 μm) was greater, being about 10 ns. It is well known that this time defines "switch on" of the strong heat non-linearity, which occurs because of heat expansion of the media under constant pressure.[38] Taking into account these two facts, one may conclude that the heat-induced non-linearity was negligibly small in our experiments. Electro-caloric effects also could not appear because the time of temperature change was too great, so that the density variation was negligible.

Table 3 Results of measurements of non-linear refractive index n_2 and third-order optical susceptibility (Re($\chi^{(3)}$)); unless stated otherwise, the test wave is linearly polarized and the pulse energy is 40 μJ

Composite[a]	n_2/cm^2 W^{-1}	Re($\chi^{(3)}$)/esu
I[b]	-5.0×10^{-12}	-2.5×10^{-10}
III	-3.5×10^{-12}	-1.7×10^{-10}
III (with circular polarization)	-2.2×10^{-12}	-1.1×10^{-10}
III (with pulse energy 10 μJ)	-3.6×10^{-12}	-1.8×10^{-10}
IV	-2.5×10^{-12}	-1.2×10^{-10}
$CHCl_3$[36]	5.0×10^{-15}	2.5×10^{-13}
Optical glasses[33]	$4–14 \times 10^{-16}$	$2–7 \times 10^{-14}$
PTS polymer[34]	5.0×10^{-12}	2.5×10^{-10}

[a] Film thickness 40 μm. [b] Z-scan measurements performed by the Bielorussian National Academy Institute of Physics group at 1054 nm with 3 ps pulses.

The striction lens was estimated also to be negligibly small for the picosecond pulses whose duration is less than the characteristic time of sound propagation across the diameter of the focussed beam. For all these reasons the measured non-linear optical susceptibility can be explained only by "fast mechanisms": the electronic or orientational types of non-linearity. Another factor supporting this conclusion is the good correlation of our measurement results for the two pulse durations of 3 ps and 40 ps.[39]

The experimental data agree well with the theoretical dependence of sample transmission. The theoretical dependence of the transmission coefficient T on the position of non-linear media relative to the lens focus position ($z = 0$) is given by the following expression:[33]

$$T = 1 - \frac{2(z/z_d)\Phi_{nl}(0)}{(1 + (z/z_d)^2)^2}, \quad (1)$$

where z is the coordinate of the sample under study along the axis of focal waist. Expression (1) shows that the dependence $T(z)$ has the same form as the "dispersion curve" with the centre of symmetry in the focus point (see, for example, curves in Fig. 21 and 22).

For the polymers we studied, the sign of the non-linear coefficient corresponded to defocussing non-linearity. This fact confirmed that non-linearity of the studied polymer films cannot be explained by orientational effects responsible for self-focussing of the Gaussian beam. The only mechanism that can explain the non-linear properties of the studied samples is an electron-type non-linearity. Non-linear optical susceptibilities of this type can be both positive and negative in sign.[34,36,40]

The linear polarization of the test beam was changed to circular in order to detect the non-linearity type (electronic or orientational). For this purpose a $\lambda/4$ plate was placed before a lens at an angle 45° towards the primary beam polarization. To confirm the electronic mechanism of non-linearity the experiment with the circularly polarized beam was made together with measurements with a linearly polarized wave (Fig. 20).

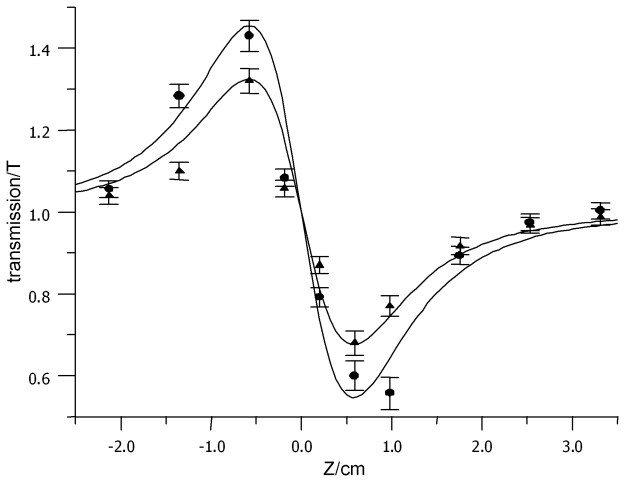

Fig. 20 Experimental data of Z-scan measurements with circular (▲) and linear (●) polarization of test beam for determination of the type of non-linearity in CrPAN film (composite **III**).

The idea was to separate isotropic electronic non-linear susceptibility $\chi^{(3)}$ with equal non-diagonal tensor compounds $\chi^{(3)}_{xyyz} = \chi^{(3)}_{xxyy} = \chi^{(3)}_{xyxy}$, and the orientational non-linear susceptibility with different values of non-diagonal compounds of the non-linear optical susceptibility tensor.[41] That is why the relations between values of the non-linear coefficient n_2 are different for waves with circular (n_{2c}) and linear (n_{2l}) polarization in media with these kinds of non-linearity. In media with electronic and orientational non-linearity this relation is $n_{2l}^{el} = 3/2\ n_{2c}^{el}$ and $-n_{2l}^{or} = 4\ n_{2c}^{or}$, respectively.[41,42] This difference between the non-linear coefficients gives rise to the essential difference in the Z-scan measurement results for beams with circular and linear polarization in these media. The ratio of ΔT values for Z-scan measurements with a beam with circular (ΔT_c) and linear (ΔT_l) polarization, determined by the ratio of n_2 values for each polarization, is different for media with electronic and orientational mechanisms of

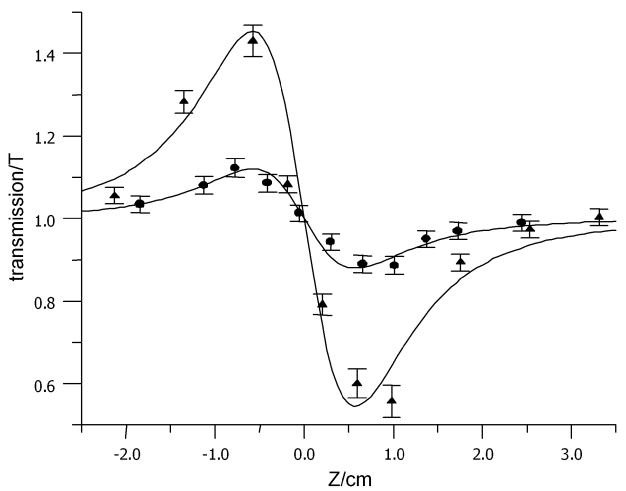

Fig. 21 Experimental results of Z-scan measurements of CrPAN polymer film (composite **III**) with pulse energy 10 μJ (●) and 40 μJ (▲).

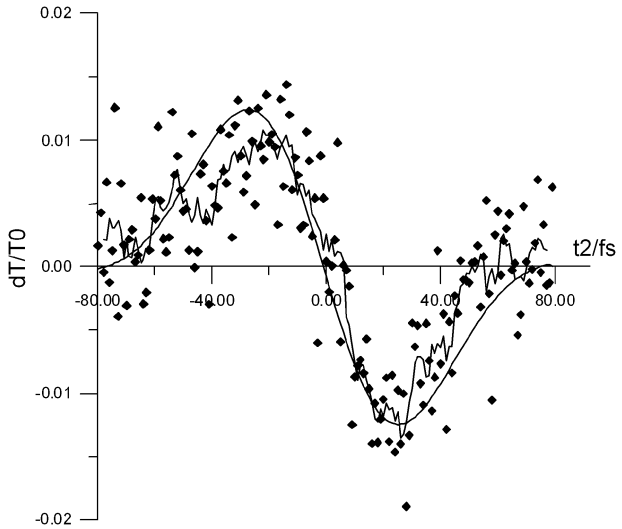

Fig. 22 Relative changes of the spectral component on varying the time delay between the pump pulse and the weak probe pulse. Experimental data points and average experimental curve compared with theoretical dependence (smooth curve) are shown for a film of composite **V**.

non-linearity. The ratios are as follows: $(\Delta T_l^{el})/(\Delta T_c^{el}) = (n_{2l}^{el})/(n_{2c}^{el}) = 3/2$ for electronic non-linearity, and $(\Delta T_l^{or})/(\Delta T_c^{or}) = (n_{2l}^{or})/(n_{2c}^{or}) = 4$ for orientational non-linearity.

Once the values of ΔT are found by experiment for each polarization of the test beam and their weighted ratio is calculated, the contribution of the electronic and orientational mechanism to the total non-linear susceptibility of the media can be found.[43] Comparison of the Z-scan measurement results for the CrPAN polymer film shown in Fig. 20 and Table 3 shows that the ratio of ΔT values for linear and circular polarizations of the test beam was $(\Delta T_l)/(\Delta T_c) = 1.5 \pm 0.4$. Consequently, in polymer films the electronic mechanism of non-linearity dominates. This fact is consistent with physical ideas about the small value of the orientational non-linearity coefficient in films, where strong interaction of molecules (molecular elasticity) impeded the reorientation of polymer molecules under the effect of the light wave electrical field.[34]

Measurements with different beam intensities were performed to check the adequacy of the Z-scan formula obtained using the approximation of small nonlinear perturbation. The results of these measurements show good correlation with measurements of the non-linear refractive index n_2 using two different values of test beam energy: 10 μJ and 40 μJ (Fig. 21).

The largest values of $\chi^{(3)}$ were found in polymer films of bis(arene)chromium-containing polyacrylonitrile -1.7×10^{-10} esu (Table 3), being much higher than for materials commonly used in non-linear optics, *e.g.* two orders of magnitude higher than for glasses.[33] Indeed, the present organometallic materials exhibit non-linear optical properties comparable to those for the best polymer materials, *e.g.* for PTS $\chi^{(3)} = 2.5 \times 10^{-10}$ esu at 1064 nm.[33]

To confirm the high level of the ultra-fast cubic refractive non-linearities of our composites, a modification of the

spectrally resolved two-beam coupling method with femtosecond laser pulses was used. The main advantages of this method are its high sensitivity compared to the Z-scan technique and the possibility of direct investigation of the ultrafast non-linearities. The principle idea is based on the detection of changes of the spectral components, shifted far from the central wavelength of the pulse, on varying the time delay between the pump pulse and the weak probe pulse.

These components have very sharp dependences on the non-linear phase shift, appearing during pulse propagation through non-linear optical media with a second strong pulse. We measured the cubic non-linear optical properties of composite **V** containing CrPAN in a PECA matrix (50 wt.%) and composite **VI** containing CrMePAN in a PECA matrix (50 wt.%). Both composites contained 3 wt.% of malonodinitrile as plastisizer, the molar ratio Cr : monomer being 8 in each case. Composites **V** and **VI** have non-linear refractive indices $n_2 = -10^{-13}$ cm^2 W^{-1} and -1.2×10^{-13} cm^2 W^{-1}, respectively. Stable results and a noise-decreasing technique allowed a decrease in the experimental error to a minimum (Fig. 22). These measurements confirmed that the test composites exhibited a significant cubic non-linear optical susceptibility of the ultra-fast electronic type also at 800 nm.

Conclusions

Novel non-linear optical polymeric film-producing nanocomposites based on bis(arene)chromium complexes incorporated into CN-containing matrices have been developed. Polymeric nanocomposite precursors were prepared by the reaction of $Cr(Et_nC_6H_{6-n})_2$ (n = 1,2,3) with CN-containing vinyl monomers (acrylonitrile, crotononitrile or ethyl 2-cyanopropenoate). Non-linear-optical conjugated structures covalently bonded with the aromatic ligands are formed in the polymeric nanocomposite precursors as a result of $(arene)_2Cr$ oxidation with air oxygen in the presence of moisture. The process of film formation involves the hydrolysis of polyacrylonitrile by the strongly alkaline $[Cr(arene)_2]^+OH^-$ species which causes the cyclization of acrylonitrile C≡N groups giving ladder-structured polynaphthyridine-type polymers with conjugated CN bonds. The comparison of the spectroscopic characteristics of free PAN after alkaline hydrolysis and those of Cr^+PAN shows a significant increase of the Stokes shift which reaches 4800 cm^{-1} for Cr^+PAN and only 2000 cm^{-1} for free PAN.

Extraodinarily high third-order non-linear optical susceptibilities of polymer films prepared from composites based on Cr^+PAN have been demonstrated using the Z-scan technique with picosecond laser pulses (with duration of 40 ps at 1064 nm and 3 ps at 1054 nm). Measurements by the spectrally resolved two-beam coupling method with a femtosecond range of pulse widths (central wavelength 795–800 nm) confirmed that the test composites exhibited a significant cubic non-linear optical susceptibility of the ultra-fast electronic type.

The electrooptical measurements of the polymer composite based on CrMePAN showed a high electrooptical response ($r_{33}n^3$ = 4.245 pm V^{-1} at modulation frequency 210 Hz and poling DC voltage 2.16 V). Also, we observed a significant enhancement of the signals with a decrease in modulation frequency. Thus, an essential contribution of orientation effects to the electro-optical response can be noted. The measurements in the absence of external electrical fields showed a "natural" anisotropy resulting from self-organization taking place during the film formation process as confirmed by the electron diffraction studies.

In CrPAN and $[CrPAN]^+TCNE^-$, a single Cr–C distance was found in the EXAFS data refinement, showing that the arene rings are parallel and symmetric as in bis(benzene) chromium. The Cr–C distances in these two materials are very similar to the 2.13 Angstroms in bis(benzene)chromium. In $[CrPAN]^+OH^-$, more than one metal–carbon distance was resolved, showing either that the two arene rings are at different distances from the metal, or that they are tilted rather than parallel. Another distance was also resolved, which is interpreted as Cr–O, showing direct coordination of the hydroxide ion to the chromium atom.

Acknowledgements

Financial support was received under Russian Foundation Grant No. 02-03-32165, the RAS Nanotechnology Programme, RF President Grant No. 8017.2006.3 and INTAS (Open Call Project 03-51-5959). We thank Professor Robert Crabtree for helpful discussions regarding the mechanism of the polycyanoethylation reaction. Access to the synchrotron facilities at the CLRC Daresbury Laboratory was awarded through the EU Framework 6 trans-national access arrangements for researchers in EU Member States and Associated States. We wish to acknowledge the assistance of Dr Fred Mosselmans during the experimental measurements at Daresbury.

References

1 G. A. Domrachev, L. G. Klapshina, V. V. Semenov, Y. A. Kurskii, A. A. Sorokin and V. N. Spektor, *Dokl. Akad. Nauk*, 1998, **358**, 782–785.
2 G. A. Domrachev, W. E. Douglas, B. Henner, L. G. Klapshina, V. V. Semenov and A. A. Sorokin, *Polym. Adv. Technol.*, 1999, **10**, 215–222.
3 G. A. Domrachev, L. G. Klapshina, V. V. Semenov, W. E. Douglas, O. L. Antipov, A. S. Kuzhelev and A. A. Sorokin, *Appl. Organomet. Chem.*, 2001, **15**, 51–55.
4 L. G. Klapshina, V. V. Semenov, Z. Y. Fominykh, G. A. Domrachev, W. E. Douglas, O. L. Antipov and A. S. Kuzhelev, *Polym. Int.*, 2002, **51**, 1178–1183.
5 A. V. Afanas'ev, A. P. Zinoviev, O. L. Antipov, B. A. Bushuk, S. B. Bushuk, A. N. Rubinov, J. Y. Fominih, L. G. Klapshina, G. A. Domrachev and W. E. Douglas, *Opt. Commun.*, 2002, **201**, 207–215.
6 N. Binstead, J. W. Campbell, S. J. Gurman and P. C. Stephenson, *EXAFS Analysis Programs*, Daresbury Laboratory, Warrington, 1991.
7 V. I. Bezrodnii, A. A. Ischenko, L. V. Karabanova and U. L. Slominskii, *Quant. Electron.*, 1995, **22**, 849.
8 I. Kang, T. Krauss and F. Wise, *Opt. Lett.*, 1997, **22**, 1077–1079.
9 A. V. Afanas'ev, A. I. Korytin, L. G. Klapshina and W. E. Douglas, *J. Opt. Technol. (Translation of Opticheskii Zhurnal)*, 2004, **71**, 608–611.
10 M. Sigelle and R. Hierle, *J. Appl. Phys.*, 1981, **52**, 4199–4204.
11 K. D. Singer, M. G. Kuzyk, W. R. Holland, J. E. Sohn, S. J. Lalama, R. B. Comizzoli, H. E. Katz and M. L. Schilling, *Appl. Phys. Lett.*, 1988, **53**, 1800–1802.

12 O. L. Antipov, A. S. Kuzhelev, A. Y. Lukyanov and A. P. Zinov'ev, *Quant. Electron.*, 1998, **28**, 867–874.
13 A. Y. Luk'yanov and A. A. Pogorelko, *Tech. Phys. (Translation of Zhurnal Tekhnicheskoi Fiziki)*, 2002, **47**, 585–590.
14 A. Y. Luk'yanov, R. V. Tyukaev, A. A. Pogorelko, E. M. Gavrishchuk and A. A. Pereskokov, *Opt. Spectrosc. (Translation of Optika i Spektroskopiya)*, 2003, **94**, 21–26.
15 M. A. Proskurnin, A. Y. Luk'yanov, S. N. Bendrysheva, A. A. Bendryshev, A. V. Pirogov and O. A. Shpigun, *Anal. Bioanal. Chem.*, 2003, **375**, 1204–1211.
16 A. Y. Luk'yanov, S. N. Bendrysheva, M. A. Proskurnin, A. A. Bendryshev, A. I. Elefterov and O. A. Shpigun, *Rev. Sci. Instrum.*, 2003, **74**, 656–658.
17 K. Katsuraya, K. Hatanaka, K. Matsuzaki and M. Minagawa, *Polymer*, 2001, **42**, 6323–6326.
18 H. P. Fritz and E. O. Fischer, *J. Organomet. Chem.*, 1967, **7**, 121–127.
19 V. Graves and J. J. Lagowsky, *Inorg. Chem.*, 1976, **15**, 577–586.
20 G. P. Karpacheva, L. M. Zemtsov, G. N. Bondarenko, A. D. Litmanovich and N. A. Plate, *Dokl. Akad. Nauk*, 1999, **368**, 354–356.
21 I. G. Rumynskaya, S. A. Agranova, E. P. Romanova and S. Y. Frenkel, *Vysokomolekulyarnye Soedineniya, Seriya A i Seriya B*, 1997, **39**, 1382–1386.
22 N. Grassie, in *Chemical Reactions of Polymers (High Polymers)*, ed. E. M. Fettes, Interscience, New York, 1964, Vol. XIX.
23 T. Takata, I. Hiroi and M. Taniyama, *J. Polym. Sci., Part A: Gen. Pap.*, 1964, **2**, 1567–1585.
24 N. S. Batty and J. T. Guthrie, *Polymer*, 1978, **19**, 1145–1148.
25 N. S. Batty and J. T. Guthrie, *Macromol. Chem. Phys.*, 1981, **182**, 71–79.
26 J. M. Manriquez, G. T. Yee, R. S. McLean, A. J. Epstein and J. S. Miller, *Science*, 1991, **252**, 1415–1417.
27 J. Weber, M. Geoffroy, A. Goursot and E. Penigault, *J. Am. Chem. Soc.*, 1978, **100**, 3995–4003.
28 T. T. T. Li, W. J. Kung, D. L. Ward, B. McCulloch and C. H. Brubaker, Jr, *Organometallics*, 1982, **1**, 1229–1235.
29 J. S. Miller, D. M. O'Hare, A. Chakraborty and A. J. Epstein, *J. Am. Chem. Soc.*, 1989, **111**, 7853–7860.
30 D. C. Koningsberger and R. Prins, *X-ray Absorption, Principles, Applications, Techniques of EXAFS, SEXAFS, and XANES*, Wiley, New York, 1988.
31 G. Meitzner, G. H. Via, F. W. Lytle and J. H. Sinfelt, *J. Phys. Chem.*, 1992, **96**, 4960.
32 A. Mustafa, M. Achilleos, J. Ruiz-Iban, J. Davies, R. E. Benfield, R. G. Jones, D. Grandjean and S. J. Holder, *React. Funct. Polym.*, 2006, **66**, 123–135.
33 R. F. Shi and A. F. Garito, in *Characterization Techniques and Tabulations for Organic Nonlinear Optical Materials*, ed. M. G. Kuzyk and C. W. Dirk, Marcel Dekker, New York-Basle-Hong Kong, 1998, pp. 1–36.
34 E. W. Van Stryland and M. Sheik-Bahae, in *Characterization Techniques and Tabulations for Organic Nonlinear Optical Materials*, ed. M. G. Kuzyk and C. W. Dirk, Marcel Dekker, New York-Basle-Hong Kong, 1998, pp. 655–692.
35 S. Kershaw, in *Characterization Techniques and Tabulations for Organic Nonlinear Optical Materials*, ed. M. G. Kuzyk and C. W. Dirk, Marcel Dekker, New York-Basle-Hong Kong, 1998, pp. 515–654.
36 H. S. Nalwa, *Adv. Mater.*, 1993, **5**, 341.
37 J. K. Frisoli, Y. Hefetz and T. F. Deutsch, *Appl. Phys. B*, 1991, **52**, 168.
38 D. Smith, *Proc. IEEE*, 1977, **65**, 76.
39 O. L. Antipov, B. A. Bushuk, G. A. Domrachev, W. E. Douglas, L. G. Klapshina, A. S. Kuzhelev, A. N. Rubinov and A. P. Zinov'ev, in *Technical Digest of CLEO/EUROPE 2000*, IEEE Service Center, Piscataway, 2000, p. 193.
40 J. Zyss, *Molecular Nonlinear Optics: Materials, Physics and Devices*, Academic Press, Boston, 1993.
41 S. Kielich, *Molekularna optyka nieliniowa*, PWN, Warsaw, 1977.
42 S. N. Vlasov and V. I. Talanov, *Wave Self-focusing*, Institute of Aplied Physics, Russian Academy of Science, Nizhny Novgorod, 1997.
43 O. L. Antipov, A. V. Afanasiev, G. A. Domrachev, W. E. Douglas, D. M. H. Guy, L. G. Klapshina and A. S. Kuzhelev, *Proc. SPIE-Int. Soc. Opt. Eng.*, 1999, **3610**, 95–102, (Laser Material Crystal Growth and Nonlinear Materials and Devices).

